ELSEVIER

Journal of Organometallic Chemistry 554 (1998) 29–40

Journal of Organometallic Chemistry

Using spectroelectrochemistry to probe the light absorbing properties of polymetallic complexes containing the tridentate bridging ligand 2,3,5,6-tetrakis(2-pyridyl)pyrazine

Sumner W. Jones, Lisa M. Vrana, Karen J. Brewer *

Department of Chemistry, Virginia Polytechnic Institute and State University, Blacksburg, VA 24061-0212, USA

Received 4 December 1996; received in revised form 12 February 1997

Abstract

The electronic structure of a series of tpp bridged ruthenium and osmium bimetallic complexes has been investigated using spectroelectrochemistry (tpp = 2,3,5,6-tetrakis(2-pyridyl)pyrazine). These chromophores are of interest since they are stereochemically defined polymetallic systems that have reasonably long-lived MLCT excited states at room temperature. The electrochemistry of these complexes displays metal based oxidations and ligand based reductions. The electronic spectroscopy is typically characterized by ligand based $\pi \rightarrow \pi^*$ and $n \rightarrow \pi^*$ transitions in the ultraviolet and metal-to-ligand charge transfer (MLCT) transitions in the visible originating from each metal and terminating on each acceptor ligand. In polymetallic systems with multiple metal centers and a wide variety of ligands, this gives rise to very complicated spectroscopy. Upon oxidation or reduction, electronic transitions involving the orbitals in the redox process are changed. This change in the electronic spectroscopy is used to aid in both electronic absorption spectroscopy and electrochemical assignments of these polymetallic complexes. With the aid of spectroelectrochemistry of this series of complexes, the nature of many of the electronic transitions of these chromophores has been elucidated. Characteristic spectroscopic changes associated with oxidation of the (tpy)M^{II}(μ-tpp) (M = Ru or Os and tpy = 2,2′,6′,2″-terpyridine) chromophore have been observed which lead to the unambiguous assignment of the metal involved in the redox process in unsymmetrical bimetallic systems. © 1998 Elsevier Science S.A.

Keywords: Spectroelectrochemistry; MLCT; Redox process

1. Introduction

Since the discovery of the light absorbing properties of $[Ru(bpy)_3]^{2+}$ (bpy = 2,2′-bipyridine), there has been much interest in transition metal complexes coordinated to polyazine ligands for use as chromophores in photochemical energy conversion schemes [1–3]. Complexes of this type can have numerous electronic transitions including metal-to-ligand charge transfer (MLCT) transitions in the visible and ligand centered $\pi \rightarrow \pi^*$ and $n \rightarrow \pi^*$ transitions in the ultraviolet. By altering the metal center or the ligands, it is possible to tune the energy of these transitions. Their typically long-lived MLCT states, coupled to this ability to tune the light absorbing properties of these systems, makes them a useful class of chromophores. Although monometallic complexes containing these chromophores have many advantageous light absorbing properties, they rely on collisional processes for quenching of their MLCT excited state. The low efficiency of these intermolecular quenching processes limits the application of these monometallic chromophores in electron or energy transfer schemes.

Many workers have used polyazine bridging ligands to construct polymetallic systems [3–32]. Bridging ligands allow the incorporation of multiple metal centers with different photophysical and chemical properties into a single molecule, thereby constructing supramolecular complexes. The most widely used bridging ligands have been of the bis-bidentate type, most notably dpp (2,3-bis(2-pyridyl)pyrazine) (for a recent review see [4]); [8–20,32].

* Corresponding author. Tel.: +1 540 2316579; Fax: +1 540 2313255; e-mail: kbrewer@chemserver.chem.vt.edu

Tris–bidentate complexes, such as $[Ru(bpy)_3]^{2+}$, exist as a mixture of Λ and Δ isomers. When the currently employed dpp type bidentate ligands are used which bind to a single metal with two nitrogen atoms that are not equivalent, additional stereoisomers occur. In multimetallic complexes, the number of possible stereoisomers can get quite large. The use of two symmetric tridentate ligands coordinated to a metal center eliminates the possibility of stereoisomers. Tridentate bridging ligands such as tpp (2,3,5,6-tetrakis(2-pyridyl)pyrazine) [4,19,20,22,23,25–30,33–35] and tpy–ph–tpy (1,4-di(2,2′,6′,2′-terpyridin-4′-yl) [21–24] have been used successfully to prepare stereochemically defined multimetallic systems.

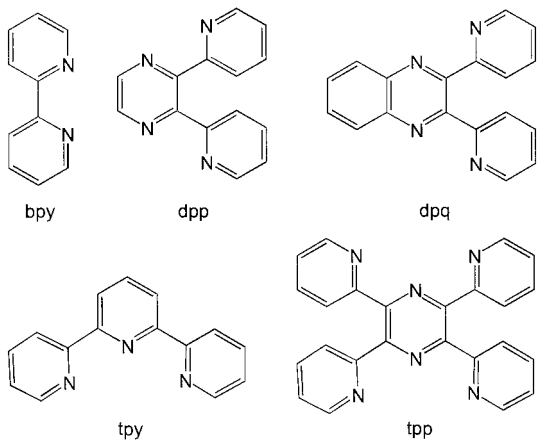

The spectroscopic and photophysical properties of a number of complexes incorporating the tridentate bridging ligand tpp have been previously reported [19,20,22,23,25–30,34,35]. Recently we have reported bimetallic, tpp-bridged complexes of Ru and Os that have long-lived MLCT states at room temperature [25]. The long MLCT excited state lifetimes of these complexes at RT results from the fact that these complexes do not have thermally accessible LF states. It is this low lying LF state that leads to the extremely short room temperature MLCT excited state lifetime of $[Ru(tpy)_2]^{2+}$ (tpy = 2,2′,6′,2′-terpyridine) [31,36–39]. The long-lived excited states, coupled to the defined stereochemistry of these tpp bridged complexes, makes them desirable chromophores for the construction of supramolecular complexes. Understanding the complicated spectroscopy and electrochemistry of these systems is essential to their successful application as chromophoric units of supramolecular assemblies.

The electronic absorption spectroscopy and electrochemistry of multimetallic complexes can be quite complicated due to the large number of electronic transitions and electroactive moieties. Typically, there is an oxidation associated with each ruthenium or osmium metal center and at least one reduction associated with each polyazine ligand. Synthetic modification aids in the interpretation of the electronic absorption spectroscopy and electrochemistry of polymetallic systems [4,6–13,17–20,25–27,35]. In this work, spectroelectrochemistry has been used to further facilitate the understanding of the complex spectroscopic and electrochemical behavior of these polymetallic systems bridged by tridentate ligands.

Spectroelectrochemistry is a powerful tool for probing the electronic transitions and electrochemical processes of metal complexes with polyazine ligands [7–15,26,40–43]. These complexes are typically described using a localized molecular orbital approach. The electrochemical oxidations are metal based and the reductions are ligand based. These same orbitals are involved in the electronic transitions. Berger used electronic absorption spectroelectrochemistry to confirm electrochemical assignments of $[(bpy)_2Ru(dpp)]^{2+}$ and $\{[(bpy)_2Ru]_2(dpp)\}^{4+}$ and to help make assignments in the excited state electronic absorption spectra of these complexes [14]. Wertz et al. used electronic absorption spectroelectrochemistry along with resonance Raman and ESR to investigate the difference in the behavior of $[(bpy)_2Ru(BL)Ru(bpy)_2]^{4+}$ (BL = dpp and dpq (2,3-bis(2-pyridyl)quinoxaline)) [15]. These two studies showed the power of spectroelectrochemistry in probing the spectroscopic and electrochemical properties of polyazine bridged polymetallic complexes. Our group has studied the spectroelectrochemistry of many bidentate bridged polyazine systems [7–13].

Although the spectroelectrochemical behavior of metal complexes containing a number of bidentate bridging ligands such as dpp has been investigated [7–15], only our preliminary report of the spectroelectrochemistry of tridentate bridging ligand, tpp based systems has appeared [26]. Reported herein is the spectroelectrochemical study of a series of complexes containing the tridentate bridging ligand tpp: $[(tpy)M(tpp)]^{2+}$, $[(tpy)Ru(tpp)Ru(tpy)]^{4+}$, $[(tpy)M(tpp)Ru(tpp)]^{4+}$, $[(tpy)M(tpp)RuCl_3]^{+}$, $[(tpy)Ru(tpp)Ru(CH_3CN)_3]^{4+}$, and $[(tpy)Ru(tpp)Ru(dpq)Cl]^{3+}$ (where $M = Os^{II}$ or Ru^{II}).

2. Experimental section

2.1. Materials

All chemicals were obtained from Aldrich Chemical Co. and used as received unless otherwise noted. Acetonitrile was obtained from Baxter Scientific. 2,3-Bis(2-pyridyl)quinoxaline was synthesized according to the methods of Goodwin and Lions [33]. 2,3,5,6-Tetra-

kis(2-pyridyl)pyrazine was purchased from GFS Chemicals. The supporting electrolyte for the electrochemistry and spectroelectrochemistry was tetrabutylammonium hexafluorophosphate, prepared by the metathesis of tetrabutylammonium bromide with potassium hexafluorophosphate, recrystallized twice from ethanol, and stored in a vacuum desiccator. Lipophilic Sephadex LH-20 size exclusion chromatography resin was obtained from Sigma. $[(tpy)Ru(tpp)](PF_6)_2$ [26], $[(tpy)Os(tpp)](PF_6)_2$ [35], $[(tpy)Ru(tpp)Ru(tpy)](PF_6)_4$ [20,27], $[(tpy)Ru(tpp)Ru(tpp)](PF_6)_4$ [25,27], $[(tpy)Os(tpp)RuCl_3](PF_6)$ [25], $[(tpy)Ru(tpp)RuCl_3](PF_6)$ [25], $[(tpy)Ru(tpp)Ru(CH_3CN)_3](PF_6)_4$ [20], and $[(tpy)Os(tpp)Ru(tpp)](PF_6)_4$ [25] were prepared as previously reported.

$[(tpy)Ru(tpp)Ru(dpq)Cl](PF_6)_3$ was synthesized by heating at reflux $[(tpy)Ru(tpp)RuCl_3](PF_6)$ (0.10 g, 0.090 mmol) and dpq (0.13 g, 0.44 mmol) in 15 ml 95% EtOH under argon for 7 h. The reaction mixture was cooled to room temperature, the crude product was precipitated by addition to 100 ml saturated aqueous KPF_6, and the product was removed by vacuum filtration. Purification was achieved by size exclusion column chromatography using a 24-inch LH-20 column with 2:1 ethanol/acetonitrile as the mobile phase. Fractions were monitored using UV-vis spectroscopy. The first part of the band to elute ($\lambda_{max} > 590$ nm with a low energy tail) was probably due to a tetrametallic complex. The second fraction ($\lambda_{max} = 586$ nm) was collected, dissolved in minimal acetonitrile, flash precipitated in diethylether, and collected by vacuum filtration. This complicated separation leads to a low yield of highly purified complex. A typical yield for this reaction was 34%.

2.2. Electrochemistry

A BioAnalytical Systems 100-W electrochemical analyzer was used to record the cyclic voltammograms and to control the electrolysis in the spectroelectrochemical experiments. The supporting electrolyte was 0.1 M Bu_4NPF_6 and the measurements were made in Burdick and Jackson UV-grade acetonitrile. The three electrode system uses a platinum disk working electrode (2.0 mm^2), a platinum wire auxiliary electrode, and a Ag/AgCl reference electrode (0.29 V vs. NHE, calibrated using the $Fe(C_5H_5)_2/Fe(C_5H_5)_2^+$ couple (0.665 V vs. NHE) [44]. All cyclic voltammograms were recorded at a scan rate of 200 mV/s without iR compensation. Typical ΔE_p were 60–80 mV.

2.3. Electronic absorption spectroscopy

Spectra were recorded at room temperature using a Hewlett Packard 8452 diode array spectrophotometer (2 nm resolution) interfaced to an IBM compatible computer. The solvent was Burdick and Jackson UV-grade acetonitrile.

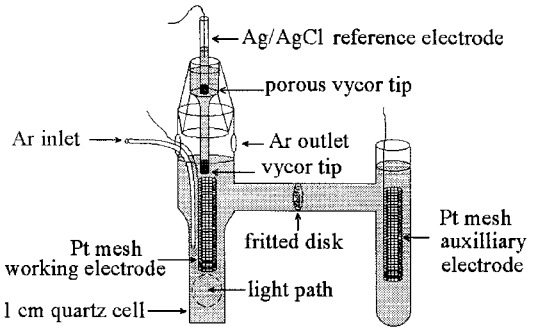

Fig. 1. Spectroelectrochemistry cell.

2.4. Spectroelectrochemistry

Electronic spectra of electrogenerated oxidized or reduced species were recorded using an H-cell as shown in Fig. 1, a modification of a previously reported cell [45]. The working compartment was a 1 cm quartz cuvette and contained the analyte in 0.1 M Bu_4NPF_6 in CH_3CN, a platinum mesh working electrode, and a Ag/AgCl reference electrode. The other compartment of the H-cell contained a platinum mesh auxiliary electrode and 0.1 M Bu_4NPF_6 in CH_3CN. The two compartments are separated by a fine porosity glass frit. The working compartment was bubbled with argon for 10 min prior to and during each experiment. The potential was controlled using a BAS 100-W electrochemical analyzer. An initial maximum absorbance of 0.6–0.8 was established. The analyte was electrochemically oxidized or reduced and the redox process monitored by UV-vis spectroscopy. All processes gave clean isosbestic points. The oxidation or reduction was considered complete when there was no further change in the UV-vis spectra ($\pm 2\%$). After the completion of the bulk electrolysis, the complex was returned electrochemically to its parent charge to determine the reversibility of the oxidation or reduction process.

3. Results and discussion

The electrochemistry of $[Ru(tpy)(tpp)](PF_6)_2$ [19,26–28], $[Os(tpy)(tpp)](PF_6)_2$ [27,35], $[(tpy)Ru(tpp)Ru(tpy)](PF_6)_4$ [19,27], $[(tpy)Ru(tpp)Ru(tpp)](PF_6)_4$ [25,27], $[(tpy)Os(tpp)Ru(tpp)](PF_6)_4$ [25], $[(tpy)Os(tpp)RuCl_3](PF_6)$ [25], and $[(tpy)Ru(tpp)RuCl_3](PF_6)$ [25], has been previously reported and is summarized in Table 1. The electrochemical behavior of these complexes is characterized by metal based oxidations and

Table 1
Electrochemistry for a series of osmium and ruthenium complexes incorporating the tridentate bridging ligand tpp[a]

Complex	$E_{1/2}$ (V)[b]		
	Oxidations	Reductions	Ref.
$[(tpy)Ru(tpp)]^{2+}$	+1.40 $Ru^{II/III}$	−0.97 $tpp^{0/-}$ −1.38 $tpy^{0/-}$ −1.60 $tpp^{-/2-}$	[19,25–28]
$[(tpy)Os(tpp)]^{2+}$	+1.06 $Os^{II/III}$	−0.97 $tpp^{0/-}$ −1.39 $tpy^{0/-}$	[27,35]
$[(tpy)Ru(tpp)Ru(tpy)]^{4+}$	+1.44 $Ru^{II/III}$ +1.76 $Ru^{II/III}$	−0.35 $tpp^{0/-}$ −0.84 $tpp^{-/2-}$ −1.30 $2tpy^{0/-}$	[19,20,27,28]
$[(tpy)\mathbf{Ru}(\mathbf{tpp})Ru(tpp)]^{4+}$	+1.51 $\mathbf{Ru}^{II/III}$ +1.86 $Ru^{II/III}$	−0.30 $\mathbf{tpp}^{0/-}$ −0.82 $\mathbf{tpp}^{-/2-}$ −1.10 $tpp^{0/-}$	[25,27]
$[(tpy)Os(\mathbf{tpp})Ru(tpp)]^{4+}$	+1.17 $Os^{II/III}$ +1.81 $Ru^{II/III}$	−0.36 $\mathbf{tpp}^{0/-}$ −0.81 $\mathbf{tpp}^{-/2-}$ −1.07 $tpp^{0/-}$	[25]
$[(tpy)\mathbf{Ru}(tpp)RuCl_3]^{+}$	+0.73 $\mathbf{Ru}^{II/III}$ +1.61 $\mathbf{Ru}^{II/III}$	−0.60 $tpp^{0/-}$ −1.10 $tpp^{-/2-}$ −1.50 $tpy^{0/-}$	[25]
$[(tpy)Os(tpp)RuCl_3]^{+}$	+0.66 $Ru^{II/III}$ +1.32 $Os^{II/III}$	−0.59 $tpp^{0/-}$ −1.07 $tpp^{-/2-}$ −1.47 $tpy^{0/-}$	[25]
$[(tpy)\mathbf{Ru}(tpp)Ru(CH_3CN)_3]^{4+}$	+1.30 $Ru^{II/III}$ +1.80 $\mathbf{Ru}^{II/III}$	−0.30 $tpp^{0/-}$ −0.80 $tpp^{-/2-}$ −1.67 $tpy^{0/-}$	[20]
$[(tpy)\mathbf{Ru}(tpp)Ru(dpq)Cl]^{3+}$	+0.87 $Ru^{II/III}$ +1.36 $\mathbf{Ru}^{II/III}$	−0.72 $tpp^{0/-}$ −1.19 $tpp^{-/2-}$ −1.42 $dpq^{0/-}$	[c]

[a] tpp, 2,3,5,6-tetrakis(2-pyridyl)pyrazine; tpy, 2,2′,6′,2′-terpyridine; dpq, 2,3-bis(2-pyridyl)benzoquinoxaline.
[b] Potentials reported in CH_3CN solution with 0.1 M TBAH and reported versus Ag/AgCl (0.29 V vs. NHE).
[c] New assignments based on this work.

ligand based reductions. For $[M(tpy)(tpp)]^{2+}$ ($M = Ru^{II}$ or Os^{II}), the oxidation is assigned as $M^{II/III}$, the first reduction is assigned as $tpp^{0/-}$, and the second reduction is assigned as $tpy^{0/-}$. This is consistent with tpp having a lower energy π^* orbital than tpy. The osmium based oxidation occurs at a less positive potential than the ruthenium based process, consistent with osmium having higher energy $d\pi$ orbitals.

Upon formation of a tpp bridged bimetallic complex, the tpp becomes easier to reduce due to a stabilization of the π^* orbital induced by the coordination of the second electron withdrawing metal center. In $[(tpy)Ru(tpp)Ru(tpy)]^{4+}$, the first two reductions are $tpp^{0/-}$ and $tpp^{-/2-}$, occurring before the $tpy^{0/-}$ reduction of both terminal tpy ligands [19,27]. The presence of a $tpp^{-/2-}$ couple prior to the reduction of the terminal tpy ligands is characteristic of the bimetallic formulation of this complex. For $[(tpy)Ru(tpp)Ru(tpy)]^{4+}$, it is notable that the two equivalent ruthenium centers oxidize at different potentials, indicating that the two metals are influenced by each other when they are bridged by the tpp ligand [19,27].

We have previously reported a series of unsymmetrical bimetallic systems bridged by tpp [25]. The order of oxidation of the metal centers is determined by the metal used and its coordination environment. Our previous assignments of their electrochemical behavior are summarized in Table 1. The spectroelectrochemical studies reported here serves to confirm these assignments.

In order to more fully understand the spectroscopy, electrochemistry, and spectroelectrochemistry of these tpp bridged complexes, we have prepared an additional system with varied ligation of the two metal centers bridged by the tpp. Substitution of two chlorides in $[(tpy)Ru(tpp)RuCl_3]^{+}$ by dpq gives $[(tpy)Ru(tpp)Ru(dpq)Cl]^{3+}$. This complex displays two well separated reversible metal oxidations and two well behaved reversible reductions. Further reduction leads to adsorption onto the electrode surface. The first oxidation, at 0.82 V, represents the oxidation of the Ru center bound to the chloride ligand since the $(tpy)Ru^{II}(tpp)$ ruthenium center is less electron rich than the $(tpp)Ru^{II}(dpq)Cl$ ruthenium center. The $(tpy)Ru^{II}(tpp)$ metal oxidation follows at 1.36 V, consistent with its coordination environment. The first reduction at −0.72 V represents the reduction of the bridging tpp ligand, i.e. $tpp^{0/-}$. The tpp ligand is expected to display a second reversible reduction, $tpp^{-/2-}$ ca. 500 mV negative of the first reduction process and this occurs at −1.19 V. The third reduction should represent the $dpq^{0/-}$ couple since the dpq ligand has lower energy π^* orbitals than tpy. This redox couple appears at −1.42 V and passing through it leads to adsorption of the analyte onto the electrode surface. The $tpy^{0/-}$ wave is expected to follow but is obscured by this adsorption process.

The electronic absorption spectroscopy for these tpp based complexes has been previously reported and is summarized in Table 2 [19,20,25–28,35]. The spectroscopy of these complexes is characterized by intense ligand $\pi \rightarrow \pi^*$ and $n \rightarrow \pi^*$ transitions in the ultraviolet and metal($d\pi$) → ligand(π^*) charge transfer transitions in the visible. Osmium based systems typically have spectroscopy that is similar to their ruthenium analogs with slight red shifts of the MLCT transitions due to the higher energy $d\pi$ orbitals of osmium. The osmium complexes also possess tails to the red of the lowest lying ^{1}MLCT and these represent the more intense ^{3}MLCT bands expected for the osmium based systems.

Table 2
Electronic absorption spectroscopy of a series of osmium and ruthenium complexes incorporating the tridentate bridging ligand tpp[a,b]

Complex	λ_{max} (nm)	Assignment	Ref.
$[Ru(tpy)(tpp)]^{2+}$	472	$Ru(d\pi) \rightarrow tpp(\pi^*)$ CT	[19,27,28]
		$Ru(d\pi) \rightarrow tpy(\pi^*)$ CT	
	354	tpp ($\pi \rightarrow \pi^*$)	[26]
	328	tpp ($\pi \rightarrow \pi^*$)	[26]
	310	$Ru(d\pi) \rightarrow tpy(\pi^*)$ CT	[c]
	290	tpp ($\pi \rightarrow \pi^*$)	[c]
	272	tpy ($\pi \rightarrow \pi^*$)	[c]
$[Os(tpy)(tpp)]^{2+}$	468	$Os(d\pi) \rightarrow tpp(\pi^*)$ CT	[27,35]
		$Os(d\pi) \rightarrow tpy(\pi^*)$ CT	
	350	tpp ($\pi \rightarrow \pi^*$)	[35]
	324	tpp ($\pi \rightarrow \pi^*$)	[35]
	314	$Os(d\pi) \rightarrow tpy(\pi^*)$ CT	[c]
	290	tpp ($\pi \rightarrow \pi^*$)	[c]
	272	tpy ($\pi \rightarrow \pi^*$)	[c]
$[(tpy)Ru(tpp)Ru(tpy)]^{4+}$	548	$Ru(d\pi) \rightarrow tpp(\pi^*)$ CT	[19,27,28]
	460	$Ru(d\pi) \rightarrow tpy(\pi^*)$ CT	[c]
	400	tpp ($\pi \rightarrow \pi^*$)	[c]
	372	tpp ($\pi \rightarrow \pi^*$)	[c]
	332	tpy ($\pi \rightarrow \pi^*$)	[c]
	298	$Ru(d\pi) \rightarrow tpy(\pi^*)$ CT	[c]
	290	tpp ($\pi \rightarrow \pi^*$)	[c]
	272	tpy ($\pi \rightarrow \pi^*$)	[c]
$[(tpy)\mathbf{Ru}(\mathbf{tpp})Ru(tpp)]^{4+}$	548	$\mathbf{Ru}(d\pi) \rightarrow \mathbf{tpp}(\pi^*)$ CT	[25,27]
		$Ru(d\pi) \rightarrow \mathbf{tpp}(\pi^*)$ CT	
	460	$\mathbf{Ru}(d\pi) \rightarrow tpy(\pi^*)$ CT	[c]
	380	**tpp** ($\pi \rightarrow \pi^*$)	[c]
	368	**tpp** ($\pi \rightarrow \pi^*$)	[c]
	340	tpp ($\pi \rightarrow \pi^*$)	[c]
	332	tpy ($\pi \rightarrow \pi^*$)	[c]
	300	$\mathbf{Ru}(d\pi) \rightarrow tpy(\pi^*)$ CT	[c]
	290	**tpp** ($\pi \rightarrow \pi^*$)	[c]
	272	tpy ($\pi \rightarrow \pi^*$)	[c]
$[(tpy)Os(\mathbf{tpp})Ru(tpp)]^{4+}$	546	$Ru(d\pi) \rightarrow \mathbf{tpp}(\pi^*)$ CT	[25]
		$Os(d\pi) \rightarrow \mathbf{tpp}(\pi^*)$ CT	
	470	$Os(d\pi) \rightarrow tpy(\pi^*)$ CT	[c]
	370	**tpp** ($\pi \rightarrow \pi^*$)	[c]
	358	**tpp** ($\pi \rightarrow \pi^*$)	[c]
	335	tpp ($\pi \rightarrow \pi^*$)	[c]
	330	tpy ($\pi \rightarrow \pi^*$)	[c]
	300	$Os(d\pi) \rightarrow tpy(\pi^*)$ CT	[c]
	290	**tpp** ($\pi \rightarrow \pi^*$)	[c]
	272	tpy ($\pi \rightarrow \pi^*$)	[c]
$[(tpy)\mathbf{Ru}(tpp)RuCl_3]^{+}$	612	$Ru(d\pi) \rightarrow tpp(\pi^*)$ CT	[25]
	525	$\mathbf{Ru}(d\pi) \rightarrow tpp(\pi^*)$ CT	[25]
	468	$\mathbf{Ru}(d\pi) \rightarrow tpy(\pi^*)$ CT	[25]
	366	tpp ($\pi \rightarrow \pi^*$)	[c]
	354	tpp ($\pi \rightarrow \pi^*$)	[c]
	332	tpy ($\pi \rightarrow \pi^*$)	[c]
	302	$\mathbf{Ru}(d\pi) \rightarrow tpy(\pi^*)$ CT	[c]
	290	tpp ($\pi \rightarrow \pi^*$)	[c]
	272	tpy ($\pi \rightarrow \pi^*$)	[c]
$[(tpy)Os(tpp)RuCl_3]^{+}$	678	$Ru(d\pi) \rightarrow tpp(\pi^*)$ CT	[25]
	606	$Os(d\pi) \rightarrow tpp(\pi^*)$ CT	[25]
	474	$Os(d\pi) \rightarrow tpy(\pi^*)$ CT	[25]
	364	tpp ($\pi \rightarrow \pi^*$)	[c]
	354	tpp ($\pi \rightarrow \pi^*$)	[c]
	330	tpy ($\pi \rightarrow \pi^*$)	[c]
	308	$Os(d\pi) \rightarrow tpy(\pi^*)$ CT	[c]
	290	tpp ($\pi \rightarrow \pi^*$)	[c]
	272	tpy ($\pi \rightarrow \pi^*$)	[c]
$[(tpy)\mathbf{Ru}(tpp)Ru(CH_3CN)_3]^{4+}$	566	$Ru(d\pi) \rightarrow tpp(\pi^*)$ CT	[20]
		$\mathbf{Ru}(d\pi) \rightarrow tpp(\pi^*)$ CT	
	464	$\mathbf{Ru}(d\pi) \rightarrow tpy(\pi^*)$ CT	[c]
	376	tpp ($\pi \rightarrow \pi^*$)	[c]
	366	tpp ($\pi \rightarrow \pi^*$)	[c]
	332	tpy ($\pi \rightarrow \pi^*$)	[c]
	300	$\mathbf{Ru}(d\pi) \rightarrow tpy(\pi^*)$ CT	[c]
	290	tpp ($\pi \rightarrow \pi^*$)	[c]
	272	tpy ($\pi \rightarrow \pi^*$)	[c]
$[(tpy)\mathbf{Ru}(tpp)Ru(dpq)Cl]^{3+}$	584	$Ru(d\pi) \rightarrow tpp(\pi^*)$ CT	[c]
		$\mathbf{Ru}(d\pi) \rightarrow tpp(\pi^*)$ CT	[c]
	565	$Ru(d\pi) \rightarrow dpq(\pi^*)$ CT	[c]
	525	$Ru(d\pi) \rightarrow tpp(\pi^*)$ CT	[c]
	460	$\mathbf{Ru}(d\pi) \rightarrow tpy(\pi^*)$ CT	[c]
	376	tpp ($\pi \rightarrow \pi^*$)	[c]
	366	tpp ($\pi \rightarrow \pi^*$)	[c]
	332	tpy ($\pi \rightarrow \pi^*$)	[c]
	296	$Ru(d\pi) \rightarrow tpy(\pi^*)$ CT	[c]
	290	tpp ($\pi \rightarrow \pi^*$)	[c]
	272	tpy ($\pi \rightarrow \pi^*$)	[c]

[a] Spectra recorded in CH_3CN at RT.
[b] tpp, 2,3,5,6-tetrakis(2-pyridyl)pyrazine; tpy, 2,2′,6′,2′-terpyridine; dpq, 2,3-bis(2-pyridyl)benzoquinoxaline.
[c] New assignments based on spectroelectrochemical studies in this work.

Spectroelectrochemistry is a technique that is used to probe the electrochemistry and electronic absorption spectroscopy of complexes that are stable in a variety of oxidation states [7–15,26,40–43]. In this experiment the complex is oxidized or reduced and the changes in the electronic absorption spectrum are monitored. This oxidation or reduction results in dramatic changes in any transitions involving the orbital that is involved in the electrochemical process. New transitions can appear as a result of a newly occupied orbital via reduction or a newly partially unoccupied orbital via oxidation. Minor shifts in transitions not involving the redox orbital can also occur. In the complexes studied, the metals can be oxidized and the polyazine ligands can be reduced. Oxidation of a metal will cause a dramatic shift in the energy of any MLCT transitions involving that metal. Metal oxidation will also tend to stabilize the π^* orbitals of the polyazine ligands coordinated to that metal, giving rise to slight red shifts in transitions involving that acceptor orbital. The reduction of the polyazine ligands in this study; tpp, tpy, and dpq, results in the electron formally residing in the π^* orbital of

that ligand. This results in a dramatic shift in the energy of any MLCT transitions involving that ligand. Ligand centered $\pi \rightarrow \pi^*$ transitions involving the reduced ligand also shift in energy. Reduction of the ligand can also cause the appearance of new ligand $\pi^* \rightarrow \pi^*$ transitions in the visible region of the spectrum.

The spectroelectrochemistry of $[Ru(tpy)(tpp)]^{2+}$, shown in Fig. 2, has been previously reported by our group but is presented here for a more detailed analysis [26]. Upon oxidation of the ruthenium metal center, a number of spectroscopic changes are evident. The loss of the band centered at 472 nm upon oxidation of Ru^{II} to Ru^{III} is consistent with the previous assignment of this transition as overlapping Ru → tpy and Ru → tpp CT transitions. Oxidation of the ruthenium would also be expected to lower the energy of the tpp π^* orbitals resulting in slight red shifts of the tpp $\pi \rightarrow \pi^*$ transitions. This effect is seen in the tpp $\pi \rightarrow \pi^*$ transitions at 328 nm and 354 nm. A peak at 310 nm is lost upon metal oxidation, consistent with a higher energy MLCT band in this region. This metal based oxidation gave > 95% regeneration of the parent complex.

When $[Ru(tpy)(tpp)]^{2+}$ is reduced by one electron, one would expect that the added electron would formally reside on the tpp π^* orbital. The loss of the peaks at 328 nm and 354 nm from this spectral region upon reduction of the complex supports the assignment of these transitions as tpp $\pi \rightarrow \pi^*$ based. Since the band at 472 nm represents overlapping Ru → tpy and Ru → tpp CT bands, this band should decrease in intensity upon tpp reduction due to the loss of the Ru → tpp CT component. Several new absorbances appear in the visible upon tpp reduction and can be attributed to new tpp $\pi^* \rightarrow \pi^*$ transitions. These new $\pi^* \rightarrow \pi^*$ based transitions obscure changes in this region. The transition at 310 nm can be assigned as a high energy Ru → tpy

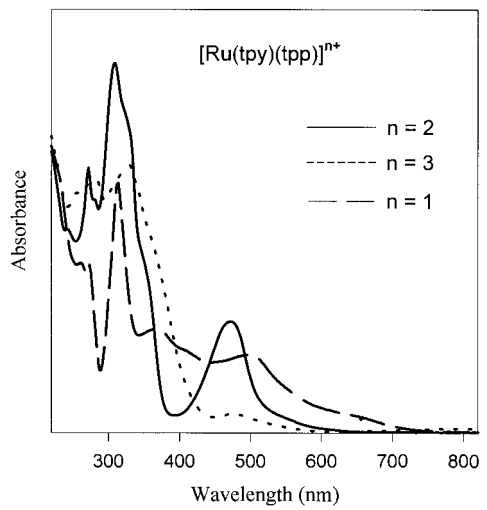

Fig. 2. Spectroelectrochemistry of $[Ru(tpy)(tpp)](PF_6)_2$ in CH_3CN (tpp = 2,3,5,6-tetrakis(2-pyridyl)pyrazine; tpy, 2,2′,6′,2″-terpyridine).

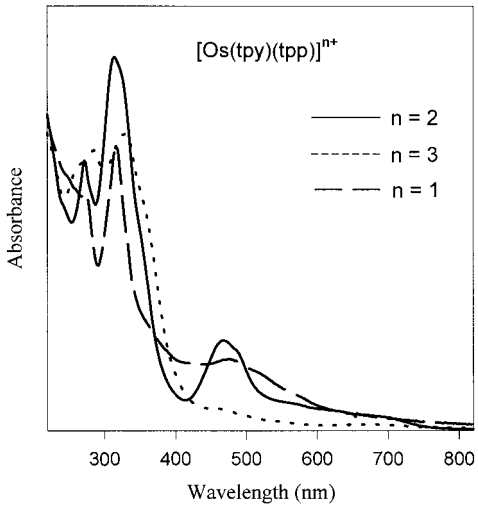

Fig. 3. Spectroelectrochemistry of $[Os(tpy)(tpp)](PF_6)_2$ in CH_3CN (tpp = 2,3,5,6-tetrakis(2-pyridyl)pyrazine; tpy = 2,2′,6′,2″-terpyridine).

CT transition since oxidation of the ruthenium causes the loss of the transition while the transition remains and slightly red shifts when the tpp is reduced. A peak is lost from the 290 nm region upon tpp reduction consistent with a higher energy tpp based $\pi \rightarrow \pi^*$ band. A peak at 272 nm remains unchanged upon metal oxidation or tpp reduction and likely represents a higher energy tpy $\pi \rightarrow \pi^*$ band. Following this reduction, the parent complex can be regenerated with > 75% efficiency.

The spectroelectrochemistry of $[Os(tpy)(tpp)]^{2+}$ is shown in Fig. 3. It was possible to generate the one electron oxidized species $[Os(tpy)(tpp)]^{3+}$ with > 95% regeneration of the parent complex. The one electron reduced species was electrogenerated with > 80% regeneration of the parent complex. The spectroelectrochemistry of this osmium chromophore is virtually identical to that observed for the previously discussed ruthenium analog. Within this bis-tridentate framework, the spectroscopy of the ruthenium and osmium analogs is remarkably similar despite the fact that the osmium metal center is substantially easier to oxidize [25,27,35]. The spectroelectrochemistry shows that this similarity in the spectroscopy of the ruthenium and osmium systems extends to their one electron oxidized and reduced forms. The 550–750 nm region of $[Os(tpy)(tpp)]^{2+}$ exhibits an increased absorbance relative to the ruthenium analog. This region represents the ^{3}MLCT bands which have higher intensity in the osmium system due to a higher degree of spin orbit coupling. Peaks in this region are lost upon osmium oxidation consistent with this ^{3}MLCT assignment.

In the following discussion of the series of bis-ruthenium complexes, a bold font will be used to indicate the ruthenium coordinated to tpy and tpp and a

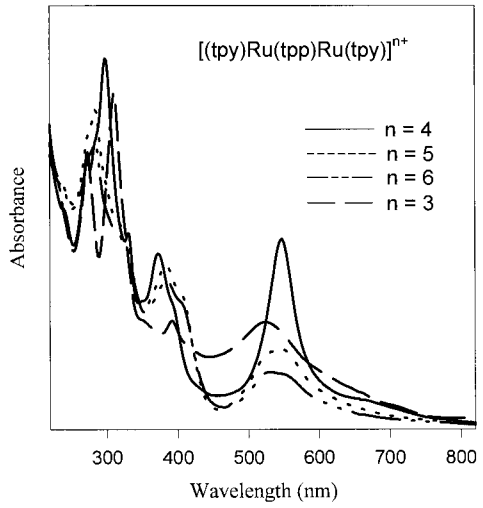

Fig. 4. Spectroelectrochemistry of $[(tpy)Ru(tpp)Ru(tpy)](PF_6)_4$ in CH_3CN (tpp = 2,3,5,6-tetrakis(2-pyridyl)pyrazine; tpy = 2,2′,6′,2″-terpyridine).

normal font will be used to indicate the other ruthenium, $[(tpy)\mathbf{Ru}(tpp)RuL_3]^{n+}$. In complexes that have two tpp ligands, a bold font will be used for the bridging tpp, $[(tpy)M(\mathbf{tpp})Ru(tpp)]^{4+}$.

The oxidative and reductive spectroelectrochemistry of $[(tpy)Ru(tpp)Ru(tpy)]^{4+}$ is shown in Fig. 4. The absorbance at 548 nm has been assigned as overlapping Ru → tpp CT transitions based on the two equivalent ruthenium centers. Oxidation of the first ruthenium metal decreases the intensity of the MLCT at 548 nm with the remaining intensity being due to the Ru → tpp CT transition involving the unoxidized ruthenium. One would expect $[(tpy)Ru(tpp)Ru(tpy)]^{4+}$ to have a Ru → tpy CT band at ca. 460 nm. A shoulder appears in this region which decreases in intensity upon metal oxidation consistent with an underlying Ru → tpy CT band. Oxidation by one electron also results in a red shift of the tpp $\pi \rightarrow \pi^*$ transitions at 372 and 400 nm and a loss of intensity in the 298 nm region. A second one electron oxidation results in further loss of the Ru → tpp CT transition at 548 nm. The 298 nm region exhibits a marked decrease in absorbance upon metal oxidation. This is consistent with a MLCT band occurring in this region and the peak at 298 nm is assigned as a higher energy Ru → tpy CT band. This loss of a peak in the 298 nm region upon generation of a $(tpy)M^{III}(tpp)$ moiety is found to be characteristic of this chromophore and can be used to assign oxidation to that particular metal center. A band at 530 nm persists after both metals have been oxidized. This could be a result of incomplete oxidation but could also be attributed to a new tpp → Ru^{III} ligand-to-metal charge transfer (LMCT) transition made possible by metal oxidation. Electrogeneration of these oxidized complexes is possible with > 95% regeneration of the parent complex.

Reduction of $[(tpy)Ru(tpp)Ru(tpy)]^{4+}$ by one electron formally reduces the tpp based π^* orbital. This results in a bleaching of the $Ru(d\pi) \rightarrow tpp(\pi^*)$ CT transitions at 548 nm, new tpp $\pi^* \rightarrow \pi^*$ transitions at 400 and 538 nm, and a loss from their original spectral region of the tpp $\pi \rightarrow \pi^*$ transitions at 372 and 400 nm. The 298 nm region is unaffected by tpp reduction consistent with the Ru → tpy CT nature of this band. A band at ca. 290 nm is lost from this spectral region upon tpp reduction but remains upon metal oxidation. This is consistent with a higher tpp $\pi \rightarrow \pi^*$ band in this region. Two peaks at 272 and 332 nm remain upon metal oxidation and tpp reduction and likely represent tpy based $\pi \rightarrow \pi^*$ bands. Electrogeneration of the one electron reduced species is reversible with > 90% regeneration of the parent complex. It was not possible to reversibly generate the two electron reduced form of this complex.

Fig. 5 contains the spectroelectrochemical results for $[(tpy)\mathbf{Ru}(\mathbf{tpp})Ru(tpp)]^{4+}$. Electrogeneration of the one electron oxidized complex is possible with > 95% regeneration of the parent complex. The band at 548 nm has been assigned as two overlapping Ru → **tpp** and **Ru** → **tpp** CT transitions involving the bridging ligand, with the lower energy component being attributed to the **Ru** → **tpp** CT transition localized on the $(tpy)\mathbf{Ru}^{II}(\mathbf{tpp})$ moiety. The first oxidation has been assigned as oxidation of the ruthenium metal that is coordinated to both tpy and tpp. Generation of the $[(tpy)\mathbf{Ru}^{III}(\mathbf{tpp})Ru^{II}(tpp)]^{5+}$ species results in the loss of the lower energy component of the band at 548 nm with the remaining intensity being due to the higher energy Ru → **tpp** MLCT transition involving the ruthenium coordinated to two tpp ligands. Oxidation of the ruthenium metal also lowers the energy of the bridging

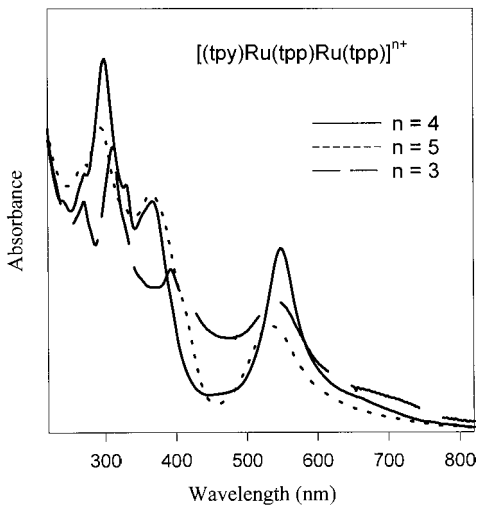

Fig. 5. Spectroelectrochemistry of $[(tpy)Ru(tpp)Ru(tpp)](PF_6)_4$ in CH_3CN (tpp = 2,3,5,6-tetrakis(2-pyridyl)pyrazine; tpy = 2,2′,6′,2″-terpyridine).

tpp π^* orbital, red shifting the $\pi \rightarrow \pi^*$ transitions at 380 and 368 nm associated with this bridging tpp. The terminal tpp should exhibit $\pi \rightarrow \pi^*$ bands in this region at ca. 340 nm that remain at the same energy upon oxidation of the (tpy)**Ru**(**tpp**) metal center. The tpy based $\pi \rightarrow \pi^*$ band at 332 nm experiences a slight red shift upon generation of the (tpy)$\mathbf{Ru}^{III}$(**tpp**) moiety. Lost is a peak at 300 nm. This is consistent with a higher energy **Ru** → tpy CT band in this region. Loss of this peak is characteristic of generation of a (tpy)Ru^{III}(tpp) center and solidifies the electrochemical assignment for this couple. Underlying **Ru** → tpy and Ru → tpp CT bands should be present in the 460–470 nm region. A loss of intensity in this region upon ruthenium oxidation indicates that these peaks are probably present. It was not possible to reversibly generate the two electron oxidized complex.

Fig. 5 also shows the reductive spectroelectrochemical results for [(tpy)**Ru**(**tpp**)Ru(tpp)]$^{4+}$. It was possible to generate the one electron reduced species with > 95% regeneration of the parent complex. When reduced by one electron, the electron formally resides on the bridging **tpp** π^* orbital and this results in the loss of both the Ru → **tpp** and the **Ru** → **tpp** CT transitions centered at 548 nm. Reduction of the bridging **tpp** results in the loss of the **tpp** $\pi \rightarrow \pi^*$ transitions at 368 and 380 nm. New **tpp** based $\pi^* \rightarrow \pi^*$ transitions appear at 550 and 400 nm upon reduction. The high energy **Ru** → tpy CT band originally at 300 nm is slightly red shifted by **tpp** reduction but a closely spaced band at ca. 290 nm is lost. This peak at 290 nm was seen to be retained upon one electron oxidation to generate the (tpy)Ru^{III}(tpp) moiety. These two observations point to a higher energy **tpp** based $\pi \rightarrow \pi^*$ transition in this 290 nm region. The peaks at 272 and 332 nm are unchanged upon metal oxidation or **tpp** reduction and can be assigned as higher energy tpy $\pi \rightarrow \pi^*$ bands. It was not possible to reversibly generate the two electron reduced species.

Fig. 6 shows the spectroelectrochemical results for [(tpy)Os(**tpp**)Ru(tpp)]$^{4+}$. Electrogeneration of the one electron oxidized complex is possible with > 95% regeneration of the parent complex. It is worth noting the very similar spectroscopy observed not only in the synthesized oxidation state of [(tpy)M(tpp)Ru(tpp)]$^{4+}$ (M = Ru^{II} or Os^{II}), but also in the electrogenerated states seen in the spectroelectrochemistry. Slight differences are observed in the 650–700 nm region with an increase in absorbance for the osmium analog. This results from the ^{3}MLCT bands occurring in this region having higher intensity for the osmium chromophore. The band at 546 nm has been assigned as overlapping Ru → **tpp** and Os → **tpp** CT transitions involving the bridging **tpp** ligand with the lower energy component being the osmium based transition. The first oxidative process has been assigned as the $Os^{II/III}$ oxidation. Electrogeneration of this state should result in a spectrum that closely matches that of the one electron oxidized species [(tpy)$\mathbf{Ru}^{III}$(**tpp**)Ru^{II}(tpp)]$^{5+}$ shown in Fig. 5. As expected, the lower energy component of the band at 546 nm in [(tpy)Os(**tpp**)Ru(tpp)]$^{4+}$ is lost upon osmium oxidation with the remaining intensity being assigned as the Ru → **tpp** CT involving the bridging **tpp** ligand. The lower energy 650–700 nm region loses intensity upon osmium oxidation due to the loss of the osmium based ^{3}MLCT transition in this region. The peak at 470 nm is lost upon osmium oxidation, consistent with a Os → tpy CT band. The $\pi \rightarrow \pi^*$ transitions of the bridging **tpp** at 358 and 370 nm are red shifted upon osmium oxidation. The tpp $\pi \rightarrow \pi^*$ bands for the terminal tpp should remain unchanged by osmium oxidation. Shoulders at 330 and 272 nm also remain upon osmium oxidation and this complex is expected to have a tpy based $\pi \rightarrow \pi^*$ bands in these regions. There is a loss of intensity at 300 nm upon osmium oxidation that can be attributed to the loss of the Os → tpy CT transition. The remaining intensity in the 290 nm region is due to the **tpp** $\pi \rightarrow \pi^*$ transition. It was not possible to reversibly generate the two electron oxidized species of this complex.

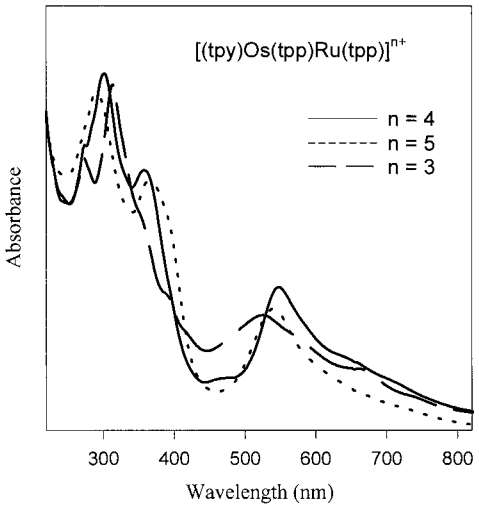

Fig. 6. Spectroelectrochemistry of [(tpy)Os(tpp)Ru(tpp)]$(PF_6)_4$ in CH_3CN (tpp = 2,3,5,6-tetrakis(2-pyridyl)pyrazine; tpy = 2,2′,6′,2″-terpyridine).

The reductive spectroelectrochemistry of [(tpy)Os(**tpp**)Ru(tpp)]$^{4+}$ is also shown in Fig. 6. It was possible to generate the one electron reduced species with > 80% regeneration of the parent complex. When reduced by one electron, the electron formally resides on the bridging **tpp** π^* orbital. This results in the loss of the Os → **tpp** and Ru → **tpp** CT transitions at 546 nm and new **tpp** $\pi^* \rightarrow \pi^*$ transitions in the visible at 400 and 540 nm. The **tpp** $\pi \rightarrow \pi^*$ transitions at 358 and 370 nm are lost upon **tpp** reduction. The higher energy terminal tpp $\pi \rightarrow \pi^*$ component at ca. 335 nm is maintained upon **tpp** reduction. As in the all ruthe-

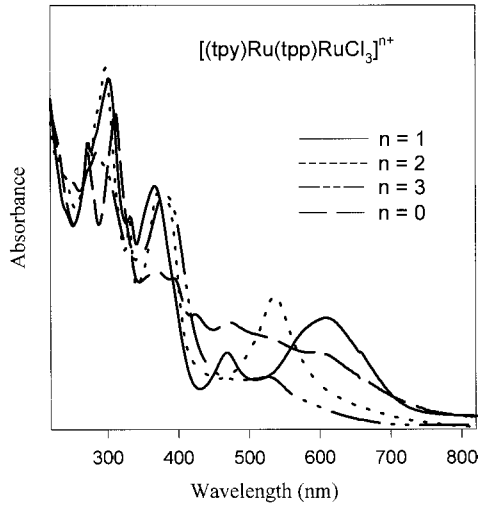

Fig. 7. Spectroelectrochemistry of $[(tpy)Ru(tpp)RuCl_3](PF_6)$ in CH_3CN (tpp = 2,3,5,6-tetrakis(2-pyridyl)pyrazine; tpy = 2,2′,6′,2″-terpyridine).

nium analog, the loss of intensity at 290 nm upon one electron reduction of $[(tpy)Os(\mathbf{tpp})Ru(tpp)]^{4+}$ is consistent with the high energy **tpp** $\pi \rightarrow \pi^*$ assignment of this transition. The tpy $\pi \rightarrow \pi^*$ bands at 272 and 330 nm are unchanged by metal oxidation or tpp reduction. It was not possible to reversibly generate the two electron reduced form of this complex.

The oxidative and reductive spectroelectrochemistry of $[(tpy)\mathbf{Ru}(tpp)RuCl_3]^+$ is shown in Fig. 7. Electrogeneration of the one and two electron oxidized species is possible with $>95\%$ regeneration of the parent complex. Upon oxidation by one electron, the ruthenium bound to three chlorides is oxidized and the absorbance at 612 nm is lost, consistent with the previous assignment of this transition as being a Ru → tpp CT transition [25]. The oxidation of Ru^{II} to Ru^{III} also stabilizes the tpp π^* orbital which should result in a red shift of the $\mathbf{Ru}(d\pi) \rightarrow tpp(\pi^*)$ CT transition. The intense band at 536 nm represents this MLCT which seems to gain significant intensity and sharpen as the ruthenium bound to three chlorides is oxidized. The **Ru** → tpy transition at 468 nm is obscured by the intense **Ru** → tpp CT transition at 536 nm in the one electron oxidized complex. Stabilization of the tpp π^* orbital upon ruthenium oxidation red shifts the tpp $\pi \rightarrow \pi^*$ transitions at 354 and 366 nm. No change in the 300 nm region is observed upon generation of the singly oxidized complex. This is consistent with a $(tpp)Ru^{III}Cl_3$ product and would be inconsistent with a $(tpy)\mathbf{Ru}^{III}(tpp)$ center. It is interesting to note that the visible portion of the spectrum for the one electron oxidized form, $[(tpy)\mathbf{Ru}^{II}(tpp)Ru^{III}Cl_3]^+$, is quite similar to the unoxidized $[(tpy)Ru(\mathbf{tpp})Ru(tpp)]^{4+}$. This indicates that the stabilizing effect on the tpp π^* orbitals of $Ru^{II}(tpp)$ binding is about equal to that of $Ru^{III}Cl_3$ binding. Oxidation of $[(tpy)\mathbf{Ru}(tpp)RuCl_3]^+$ by a second electron results in the loss of absorbances at 536 and 468 nm, consistent with **Ru** → tpp and **Ru** → tpy CT transitions, respectively. The oxidation of this **Ru** would also be expected to lead to the observed loss of the higher energy **Ru** → tpy CT transition at 302 nm. The peaks at 332 and 272 nm are maintained upon Ru oxidation and slightly red shifted upon **Ru** oxidation consistent with a tpy $\pi \rightarrow \pi^*$ assignment.

The reductive spectroelectrochemistry of $[(tpy)\mathbf{Ru}(tpp)RuCl_3]^+$ is also shown in Fig. 7. The one electron reduced species is produced with $>75\%$ regeneration of the parent complex. The one electron reduction of $[(tpy)\mathbf{Ru}(tpp)RuCl_3]^+$ would result in the electron formally residing on the tpp π^* orbital. The loss of the peaks at 354 and 366 nm is consistent with the assignment of tpp $\pi \rightarrow \pi^*$ transitions. Loss of the band at 612 nm upon reduction of tpp is consistent with this absorbance being due to the Ru → tpp CT transition. New tpp $\pi^* \rightarrow \pi^*$ transitions are expected in the visible and obscure changes to this region. A peak at 290 nm is lost upon tpp reduction consistent with a higher energy tpp based $\pi \rightarrow \pi^*$ band occurring in this region. The bands at 272 and 332 nm remain unchanged upon metal oxidation or tpp reduction consistent with their tpy $\pi \rightarrow \pi^*$ assignment. It was not possible to reversibly reduce this complex by two electrons.

Fig. 8 shows the spectroelectrochemical results for $[(tpy)Os(tpp)RuCl_3]^+$. It was possible to generate the one electron oxidized species with $>75\%$ regeneration of the parent complex. The first oxidation for this complex has been assigned as the $Ru^{II/III}$ couple and the second as the $Os^{II/III}$ couple. Oxidation of the ruthenium should lead to the loss of the ruthenium based MLCT transitions. The one electron oxidation

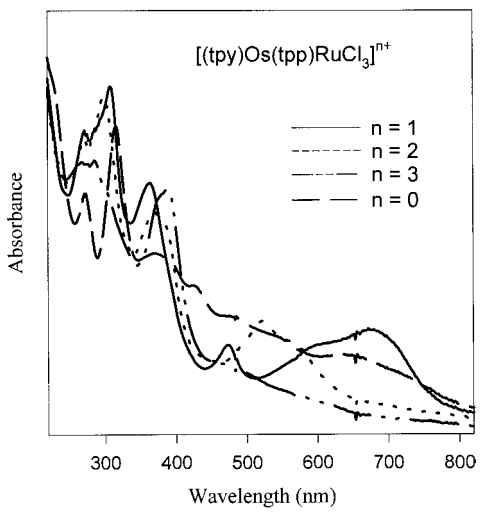

Fig. 8. Spectroelectrochemistry of $[(tpy)Os(tpp)RuCl_3](PF_6)$ in CH_3CN (tpp = 2,3,5,6-tetrakis(2-pyridyl)pyrazine; tpy = 2,2′,6′,2″-terpyridine).

results in a loss of the band at 678 nm, verifying the assignment of this band as a Ru → tpp CT transition. The peak at 606 nm in the parent complex has been assigned as a Os → tpp CT band and is relatively unaffected upon ruthenium oxidation. The Os → tpy CT band at 474 nm is still present in the one electron oxidized species although it is somewhat obscured by the peak at 522 nm that grows in intensity in this $[(tpy)Os^{II}(tpp)Ru^{III}Cl_3]^{2+}$ form. The tpp based $\pi \rightarrow \pi^*$ bands at 354 and 364 nm shift to lower energy upon ruthenium oxidation as expected. No change in the 308 nm region is observed upon one electron oxidation of $[(tpy)Os^{II}(tpp)Ru^{II}Cl_3]^{1+}$. This verifies the ruthenium nature of this oxidative process since this is inconsistent with a $[(tpy)Os^{III}(tpp)Ru^{II}Cl_3]^{2+}$ product. The peak at 606 nm is lost upon oxidation by two electrons to generate an oxidized osmium center. This is consistent with the assignment of this being peak being an Os → tpp CT transition. The Os → tpy CT band at 474 nm is also lost as expected upon osmium oxidation. The band at 522 nm that gains intensity upon ruthenium oxidation is lost upon osmium oxidation. This is consistent with an Os → tpp CT assignment. A peak at ca. 300 nm is also lost upon osmium oxidation and represents a high energy Os → tpy CT transition. Shoulders at 330 and 272 nm are relatively unchanged by metal oxidation consistent with tpy based $\pi \rightarrow \pi^*$ bands in this region.

In the one electron reduced form of $[(tpy)Os(tpp)RuCl_3]^+$, also shown in Fig. 8, the electron formally resides on the tpp π^* orbital. The one electron reduced complex was generated with > 75% regeneration of the parent complex. As in the Ru/Ru analog, this results in a loss of the tpp $\pi \rightarrow \pi^*$ transitions at 354 and 364 nm from this spectral region. Generation of the one electron reduced complex leads to a loss of the Ru → tpp and Os → tpp CT transitions at 678 and 606 nm, helping to solidify these assignments. Other changes in the visible region of the spectrum are obscured by new tpp $\pi^* \rightarrow \pi^*$ transitions that appear upon tpp reduction. A peak at 290 nm is lost upon tpp reduction and represents a higher energy tpp based $\pi \rightarrow \pi^*$ transition. The bands at 272 and 330 nm are unchanged upon metal oxidation or tpp reduction consistent with tpy $\pi \rightarrow \pi^*$ transitions. It was not possible to reversibly generate the two electron reduced species.

Fig. 9 shows the oxidative and reductive spectroelectrochemistry of $[(tpy)\mathbf{Ru}(tpp)Ru(CH_3CN)_3]^{4+}$. Electrogeneration of the one and two electron oxidized species is possible with > 95% regeneration of the parent complex. Upon one electron oxidation, Ru is oxidized. This bleaches the Ru → tpp CT transition at 566 nm. The absorbance at 526 nm that remains is due to the higher energy **Ru** → tpp CT component. The tpp $\pi \rightarrow \pi^*$ transitions at 366 and 376 nm are red shifted from the parent compound upon Ru oxidation. No changes in the ultraviolet are observed upon generation of this

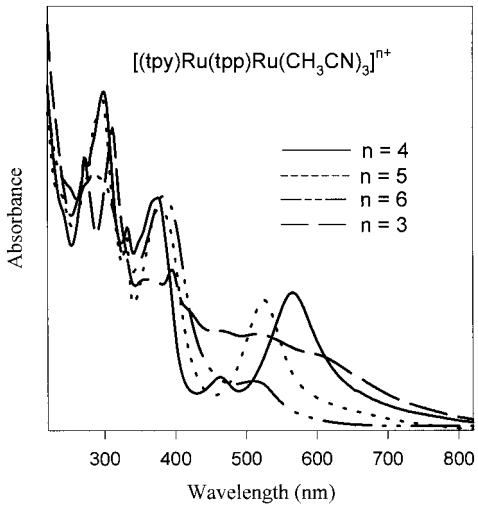

Fig. 9. Spectroelectrochemistry of $[(tpy)Ru(tpp)Ru(CH_3CN)_3](PF_6)_4$ in CH_3CN (tpp = 2,3,5,6-tetrakis(2-pyridyl)pyrazine; tpy = 2,2′,6′,2″-terpyridine).

$(tpp)Ru^{III}(CH_3CN)_3$ moiety. This clearly establishes the first oxidation of this complex as based on the ruthenium bound to the three acetonitriles since generation of a $(tpy)Ru^{III}(tpp)$ moiety has been shown above to result in changes in the 300 nm region. When $[(tpy)Ru(tpp)Ru(CH_3CN)_3]^{4+}$ is oxidized by two electrons, both ruthenium are now oxidized. The **Ru** → tpp CT transition at 526 nm is lost. The tpp based $\pi \rightarrow \pi^*$ transitions originally at 366 and 376 nm experience a slight additional red shift as the second ruthenium metal center is oxidized. A peak at ca. 300 nm is lost upon generation of the $(tpy)Ru^{III}(tpp)$ moiety consistent with a higher energy Ru → tpy CT assignment. The peaks at 272 and 332 nm are relatively unaffected by metal oxidation and represent tpy $\pi \rightarrow \pi^*$ bands.

The reductive spectroelectrochemistry of $[(tpy)\mathbf{Ru}(tpp)Ru(CH_3CN)_3]^{4+}$ is shown in Fig. 9. Electrogeneration of the one electron reduced species is possible with > 75% regeneration of the parent complex. When reduced by one electron, the electron formally resides in the tpp π^* orbital causing the loss of the tpp $\pi \rightarrow \pi^*$ transitions at 366 and 376 nm. The **Ru** → tpy CT transition at 300 nm is still evident after reduction of tpp, indicating that tpy serves as the acceptor ligand for this transition. A peak at 290 nm is lost upon tpp reduction and most likely represents a higher energy tpp based $\pi \rightarrow \pi^*$ transition. The reduction of tpp also causes the appearance of new tpp $\pi^* \rightarrow \pi^*$ transitions at ca. 400 and 540 nm, partially obscuring other changes in the visible region of the spectrum. It is still evident that the peak at 566 nm is lost upon tpp reduction, consistent with the assignment of **Ru** → tpp and Ru → tpp CT bands in this region. The bands at 272 and 332 nm are unchanged upon metal oxidation or tpp reduction and can be assigned as tpy $\pi \rightarrow \pi^*$ transi-

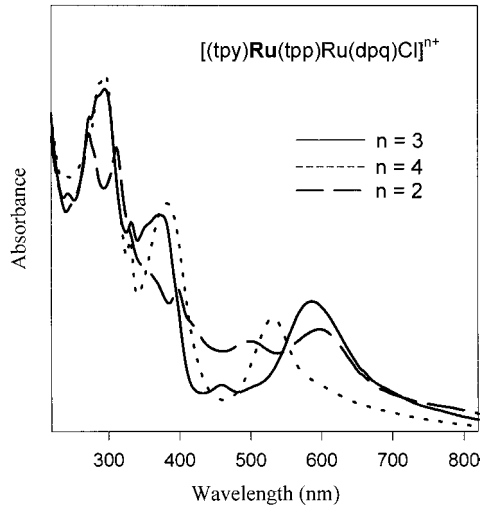

Fig. 10. Spectroelectrochemistry of $[(tpy)Ru(tpp)Ru(dpq)Cl](PF_6)_3$ in CH_3CN (tpp = 2,3,5,6-tetrakis(2-pyridyl)pyrazine; tpy = 2,2′,6′,2″-terpyridine; dpq = 2,3-bis(2-pyridyl)quinoxaline).

tions. It was not possible to reversibly generate the two electron reduced species.

The oxidative spectroelectrochemistry of $[(tpy)\mathbf{Ru}(tpp)Ru(dpq)Cl]^{3+}$ is shown in Fig. 10. Electrogeneration of the one electron oxidized species is possible with $>95\%$ regeneration of the parent complex. Oxidation by one electron oxidizes the ruthenium bound to dpq and Cl. This bleaches the low energy Ru → tpp CT band at 584 nm and the Ru → dpq CT band at 565 nm. The **Ru** → tpp CT transition at 525 nm increases in intensity as the other metal center is oxidized and the **Ru** → tpy CT band at 460 nm becomes buried in this more intense **Ru** → tpp CT peak. As with the other compounds, oxidation of one metal center lowers the energy of the tpp π^* orbital which can be seen in a red shift of the tpp $\pi \rightarrow \pi^*$ transitions at 366 and 376 nm. The ultraviolet region of the spectrum is not affected by the generation of the $(tpp)Ru^{III}(dpq)Cl$ moiety establishing the first oxidation as oxidation of this ruthenium center since generation of a $(tpy)Ru^{III}(tpp)$ moiety has been shown above to dramatically alter the 300 nm region of the spectrum. It was not possible to reversibly generate the two electron oxidized species.

The reductive spectroelectrochemistry of $[(tpy)\mathbf{Ru}(tpp)Ru(dpq)Cl]^{3+}$ is shown in Fig. 10. Electrogeneration of the one electron reduced species is possible with $>80\%$ regeneration of the parent complex. When the complex is reduced by one electron, the electron formally resides on the tpp π^* orbital resulting in the loss of the Ru → tpp and **Ru** → tpp CT transitions at 584 nm and the tpp based $\pi \rightarrow \pi^*$ transitions at 366 and 376 nm. The Ru → dpq CT transition at 565 nm remains upon tpp reduction and is slightly red shifted, as expected. Other changes in the visible portion of the spectrum are obscured by new tpp $\pi^* \rightarrow \pi^*$ transitions which have typically appeared at ca. 400 and 540 nm upon reduction of a bridging tpp. As expected, the **Ru** → tpy CT transition at 460 nm is slightly red shifted upon tpp reduction. A peak at 290 nm is lost from this spectral region upon tpp reduction consistent with a higher energy tpp based $\pi \rightarrow \pi^*$ transition occurring in this region. Loss of this peak uncovers a transition at 296 nm which in similar complexes appears to be a higher energy Ru → tpy CT band. The peaks at 272 and 332 nm are relatively unaffected by metal oxidation and tpp reduction and represent tpy $\pi \rightarrow \pi^*$ bands. It was not possible to reversibly generate the two electron reduced species.

4. Conclusions

Multimetallic complexes bridged by polyazine bridging ligands can have extremely complicated electronic absorption spectroscopy owing to the large number of MLCT and ligand centered $\pi \rightarrow \pi^*$ transitions possible. Spectroelectrochemistry has been used here to aid in the assignment of the electronic absorption spectra of the tpp-bridged complexes studied. All the bimetallic complexes studied were stable in several oxidation states and interpretation of their spectroscopy in these states uncovered several characteristic electronic absorption transitions. In the general formula for the bimetallic complexes studied, $[(tpy)M(tpp)Ru(LLL)]^{n+}$ (where M = Os^{II} or Ru^{II}, LLL = $3Cl^-$, $3CH_3CN$, tpy, tpp, or dpq and Cl^-), the lowest lying band is typically overlapping Ru → tpp and M → tpp CT transitions in the 540 to 650 nm region which is partially lost by oxidation of one metal center and completely lost upon oxidation of both metal centers. The energy of this transition varies as a function of the identity of the LLL ligands. There is also a M → tpy CT transition in the 460 to 480 nm region that is lost upon oxidation of M. The bridging tpp typically has three $\pi \rightarrow \pi^*$ transitions, two in the 350 to 380 nm region and one at ca. 290 nm. All three of these $\pi \rightarrow \pi^*$ bands are red shifted upon metal oxidation and are lost from this spectral region upon one electron reduction of each complex since this redox process is tpp π^* based. There is a M → tpy CT band at ca. 300 nm that is lost upon M oxidation. This property is very useful in determining which metal center is oxidized first in the mixed-ligand bimetallic complexes studied. Two tpy $\pi \rightarrow \pi^*$ bands at ca. 272 and 320–330 nm can be seen that are not lost by oxidation or reduction of the complex. Spectroelectrochemistry has proved very useful in probing the spectroscopy of these interesting chromophores. The spectroscopy of the oxidized and reduced forms of these complexes generated in these studies will also be useful in understanding the excited state spectroscopy of these

complexes [46] These tpp bridged polymetallic chromophores are of interest due to their long-lived MLCT excited states [25,26,35]. These and related chromophores are being utilized by our group in the construction of molecular devices for photoinitiated charge separation and electron collection [47].

Acknowledgements

We would like to thank the National Science Foundation (CHE-9313642 and CHE-9632713) for their generous support of this research and Johnson Matthey, an Alfa AESAR company, for the generous loan of ruthenium trichloride used in these studies.

References

[1] A. Juris, V. Balzani, F. Barigelletti, S. Campagna, P. Belser, A. von Zelewsky, Coord. Chem. Rev. 84 (1988) 85.
[2] K. Kalyanasundaram, Coord. Chem. Rev. 46 (1982) 159.
[3] (a) T.J. Meyer, Pure Appl. Chem. 58 (1986) 1576. (b) B. Durham, J.V. Caspar, J.K. Nagle, T.J. Meyer, J. Am. Chem. Soc. 104 (1982) 4803. (c) G.F. Strouse, J.R. Schoonover, R. Duesing, S. Boyde, W.E. Jones, T.J. Meyer, Inorg. Chem. 34 (1995) 473. (d) P.A. Anderson, G.F. Strouse, J.A. Treadway, F.R. Keene, T.J. Meyer, Inorg. Chem. 33 (1994) 3863.
[4] V. Balzani, A. Juris, M. Venturi, S. Campagna, S. Serroni, Chem. Rev. 96 (1996) 759.
[5] (a) V. Balzani, F. Scandola, Supramolecular Photochemistry, Horwood, Chichester, 1991. (b) V. Balzani, L. Moggi, F. Scandola, in: V. Balzani (Ed.), Supramolecular Photochemistry, Reidel, Dordrecht, 1987, p. 1. (c) V. Balzani, A. Credi, F. Scandola, Nato ASI Series (1994) Transition Metals in Supramolecular Chemistry, Kluwer, Dordrecht, p. 1.
[6] (a) S. Campagna, G. Denti, L. Sabatino, S. Serroni, M. Ciano, V. Balzani, Gazz. Chim. Ital. 119 (1989) 415. (b) A. Juris, V. Balzani, S. Campagna, G. Denti, S. Serroni, G. Frei, H.U. Gudel, Inorg. Chem. 33 (1994) 1491. (c) G. Denti, S. Campagna, L. Sabatino, M. Ciano, V. Balzani, Inorg. Chem. 29 (1990) 4750. (d) S. Campagna, G. Denti, S. Serroni, A. Juris, M. Venturi, V. Ricevuto, V. Balzani, Chem. Eur. J. 1 (1995) 211. (e) A. Juris, M. Venturi, L. Pontoni, I. Resino, V. Balzani, S. Serroni, S. Campagna, G. Denti, Can J. Chem. 73 (1995) 1875.
[7] S.M. Molnar, G. Nallas, J.S. Bridgewater, K.J. Brewer, J. Am. Chem. Soc. 116 (1994) 5206.
[8] S.M. Molnar, G.E. Jensen, L.M. Vogler, S.W. Jones, L. Laverman, J.S. Bridgewater, M.M. Richter, K.J. Brewer, J. Photochem. Photobiol. A:Chem. 80 (1994) 315.
[9] M.M. Richter, K.J. Brewer, Inorg. Chem. 32 (1993) 5762.
[10] M.M. Richter, G.E. Jensen, K.J. Brewer, Inorg. Chim. Acta 230 (1995) 35.
[11] M.M. Richter, K.J. Brewer, Inorg. Chem. 32 (1993) 2827.
[12] M.M. Richter, K.J. Brewer, Inorg. Chem. 31 (1992) 1594.
[13] J.S. Bridgewater, L.M. Vogler, S.M. Molnar, K.J. Brewer, Inorg. Chim. Acta 208 (1993) 179.
[14] R.M. Berger, Inorg. Chem. 29 (1990) 1920.
[15] J.B. Cooper, D.B. MacQueen, J.D. Petersen, D.W. Wertz, Inorg. Chem. 29 (1990) 3701.
[16] (a) C.H. Braunstein, A.D. Baker, T.C. Strekas, H.D. Gafney, Inorg. Chem. 23 (1984) 857. (b) Y. Fuchs, S. Lofters, T. Dieter, W. Shi, S. Morgan, T.C. Strekas, H.D. Gafney, A.D. Baker, J. Am. Chem. Soc. 109 (1987) 2691.
[17] W.R. Murphy Jr., K.J. Brewer, G. Gettliffe, J.D. Petersen, Inorg. Chem. 28 (1989) 81.
[18] A.W. Wallace, W.R. Murphy Jr., J.D. Petersen, Inorg. Chim. Acta 166 (1989) 47.
[19] J.D. Petersen, in: V. Balzani (Ed.), Supramolecular Photochemistry, Reidel, Dordrecht, 1987, p. 1135.
[20] L.M. Vogler, S.W. Jones, G.E. Jensen, R.G. Brewer, K.J. Brewer, Inorg. Chim. Acta (1997) in press.
[21] Y. Liang, R.H. Schmehl, J. Chem. Soc. Chem. Commun. (1995) 1007.
[22] E.C. Constable, A.M.W. Cargill Thompson, J. Chem. Soc. Dalton Trans. (1995) 615.
[23] J.-P. Collin, P. Laine, J.-P. Launay, J.-P. Sauvage, A. Sour, J. Chem. Soc. Chem. Commun. (1993) 434.
[24] M.T. Indelli, F. Scandola, J.-P. Collin, J.-P. Sauvage, A. Sour, Inorg. Chem. 35 (1996) 303.
[25] L.M. Vogler, K.J. Brewer, Inorg. Chem 35 (1996) 818.
[26] L.M. Vogler, B. Scott, K.J. Brewer, Inorg. Chem. 32 (1993) 898.
[27] C.R. Arana, H.D. Abruna, Inorg. Chem 32 (1993) 194.
[28] R.P. Thummel, S. Chirayil, Inorg. Chim. Acta 154 (1988) 77.
[29] R. Ruminski, J. Kiplinger, T. Cockroft, C. Chase, Inorg. Chem. 28 (1989) 370.
[30] J.-P. Sauvage, J.-P. Collin, J.-C. Chambron, S. Guillerez, C. Coudret, Chem. Rev. 94 (1994) 993.
[31] J.-P. Collin, S. Guillerez, J.-P. Sauvage, F. Barigelletti, L. De Cola, L. Flamigni, V. Balzani, Inorg. Chem. 30 (1991) 4230.
[32] J.D. Petersen, W.R. Murphy Jr., R. Sahai, K.J. Brewer, R.R. Ruminski, Coord. Chem. Rev. 64 (1985) 261.
[33] H.A. Goodwin, F. Lions, J. Am. Chem. Soc. 81 (1959) 6415.
[34] R. Ruminski, C. Letner, Inorg. Chim. Acta 162 (1989) 175.
[35] R.G. Brewer, G.E. Jensen, K.J. Brewer, Inorg. Chem. 33 (1994) 124.
[36] J.R. Kirchhoff, D.R. McMillin, P.A. Marnot, J.-P. Sauvage, J. Am. Chem. Soc. 107 (1985) 1138.
[37] J.R. Winkler, T.L. Netzel, C. Creutz, N. Sutin, J. Am. Chem. Soc. 109 (1987) 2381.
[38] R.C. Young, J.K. Nagle, T.J. Meyer, D.G. Whitten, J. Am. Chem. Soc. 100 (1978) 4773.
[39] C.R. Hecker, A.K.I. Gushurst, D.R. McMillin, Inorg. Chem. 30 (1991) 538.
[40] R.M. Berger, D.R. McMillin, Inorg. Chem. 27 (1988) 4245.
[41] (a) R.J. Donohoe, C.D. Tait, M.K. DeArmond, D.W. Wertz, J. Phys. Chem. 90 (1986) 3923. (b) R.J. Donohoe, C.D. Tait, M.K. DeArmond, D.W. Wertz, J. Phys. Chem. 90 (1986) 3927.
[42] P. Bugnon, R.E. Hester, Chem. Phys. Lett. 102 (1983) 537.
[43] G.A. Heath, L.J. Yellowlees, P.S. Braterman, J. Chem. Soc. Chem. Commun. (1981) 287.
[44] T. Gennett, D.F. Milner, M.J. Weaver, J. Phys. Chem. 89 (1985) 2787.
[45] K.J. Brewer, M. Calvin, R.S. Lumpkin, J.W. Otvos, L.O. Spreer, Inorg. Chem. 28 (1989) 4446.
[46] S.W. Jones, J.-D. Lee, K.J. Brewer, work in progress.
[47] S.W. Jones, J.A. Clark, K.J. Brewer, work in progress.